Statistical simulation of transspectral processes: LIF reabsorption

G.M. Krekov, M.M. Krekova, A.A. Lisenko, and G.G. Matvienko

V.E. Zuev Institute of Atmospheric Optics,
Siberian Branch of the Russian Academy of Sciences, Tomsk

Received September 1, 2008

This paper continues a thematic series of authors' publications, in which the statistical model of transfer of the laser-induced fluorescence (LIF) broadband radiation has been developed. Recently, the LIF phenomenon has determined the physical basis for the development of new methods of lidar sensing of vegetation and specific forms of organic aerosol, containing active fluorophores. Spectra of the chlorophyll (Chl) fluorescence emission $I_F(\lambda)$ are an important source of information about structural and functional properties of the photosynthetic apparatus. However, the shape of intrinsic fluorophore emission in most cases strongly differs due to optical distortion effects on the sample level (e.g., fluorescence reabsorption, secondary fluorescence, inner filter, surface and subsurface reflections). Particularly, the fluorescence reabsorption, caused by the overlapping of absorption and fluorescence emission spectra, generally distorts the shape of $I_F(\lambda)$. This effect was modeled by the Monte Carlo methods for homogeneous and heterogeneous plant tissues and results were compared with experimental data. Some results of numerical simulations give the foundation for creation of new methodology of the fluorescent bioaerosol distant detection in lower troposphere.

Introduction

Modern tendencies in the development of the technique for laser sensing of the atmosphere, ocean, and underlying surface are related with the use of information properties of transspectral linear and non-linear processes, accompanying the propagation of pulses of the optical radiation.[1–4] Among linear processes, which are considered in this paper, the spontaneous Raman scattering and laser-induced fluorescence are the most significant.

The urgency of the problem is caused by the fact that the laser-induced fluorescence (LIF) as an optical phenomenon gives the basis for creation of high-sensitive tools for revealing and control for a wide group of molecular compounds, including dangerous for the environment. However, adequate quantitative interpretation of LIF spectra of the chlorophyll, as well as of other possible pigments, depends on taking into account a number of distorting factors. First of all, they are noises of the atmospheric channel, which are considered in detail in Refs. 4–7. Optical distortions of the signal spectrum at the level of the initial object, i.e., a leaf, are also significant.

The spectrum of fluorescence of the leaf cover is specified, as is known,[8,9,23] by two characteristic bands of emission, the first of which $I_R(\lambda)$ is located in the red part of the visible spectrum with the center in the region of $\lambda = 670–690$ nm, and the another is in the near infrared range $I_{IR}(\lambda)$ within $\lambda = 730–740$ nm. The ratio of the LIF intensities (I_R/I_{IR}) is widely used as the index, characterizing the content of chlorophyll in a leaf and its correlations with the environment (temperature, season, technogenic stress, etc.).[9,10] However, apart from the aforementioned external factors, the magnitude of (I_R/I_{IR}) in each specific case depends on the inner photochemical processes in the leaf volume. Among these processes, the reabsorption[11] and the inter-molecular energy transfer[10,12,14] play the most important role.

The reabsorption phenomenon, on which we concentrate our attention in this paper, follows from the physically stipulated fact that the fluorescent emission generated by the chlorophyll *b* molecules in the chloroplast, has a chance to undergo the secondary absorption and reemission by other types of the chlorophyll molecule, for example, *a* and *c*, at the output of the leaf volume. Since the overlapping of the chlorophyll *b* emission spectra and the chlorophyll *a* absorption spectrum, in particular, is higher in the red wavelength range, the I_R value, recorded *in vivo* beyond the leaf, uncontrollably decreases. This inevitably leads to false conclusions about variations of the chlorophyll content. In this connection, the problem of estimation of the LIF signal transformation scales in the actual scheme of the laser sensing of vegetative cover due to distorting effect of re-absorption processes in the volume of individual leaf. This problem is considered below in the framework of the rigorous theory of radiation transfer. The principal difference between our approach from the known works[25] by Knyazikhin and Marshak lies in the fact that an individual leaf within the vegetative cover is considered not as a discrete scattering element with known generalized scattering and transmission functions, but as a local

volume with its own polydispersed structure. This requires certain modification of the mathematical model of the radiation transfer.

1. Optical model of medium

It is supposed that monochromatic radiation of fluorescent lidar at a wavelength of excitation λ is incident on a plane layer of vegetative cover located at the distance H_0. Optical-geometric parameters of the lidar (the angle of the laser beam divergence φ_s, the angle of the receiving telescope field of view φ_d, the telescope diameter S, etc) correspond to the real prototype.[13,15] The real atmosphere including local vegetative elements is a multiphase disperse medium, which can be characterized by some effective extinction coefficient $\beta_{ext}(\lambda)$. The values of $\beta_{ext}(\lambda)$ were estimated from the accompanying measurements of the elastic backscattering signals. For the deciduous forest (birch) they are within $\beta_{ext}(\lambda) = 0.15–0.25$ m^{-1} at $\lambda = 532$ nm of the second harmonic of Nd:YAG laser.[13,16] These values were accepted as the parameters of a given model experiment.

Physically, the effective extinction coefficient combines the extinction coefficients of the surrounding medium (haze, fog) $\beta_a(\lambda)$, the extinction in the volume of each vegetative element $\beta_e(\lambda)$, effects of mutual shadowing of leaves, branches, and trunks of trees $\beta_s(\lambda)$. We neglect the effect of branches and trunks, relying on conditions of the conducted natural experiments,[13,15] i.e., the optical model of the medium is considered as the plane-parallel volume of the atmospheric aerosol, chaotically filled only with leaves as elementary optical objects. The study of a leaf as an active optical object is an independent problem with its own prehistory (see, for example, Ref. 17). In a given case we attract the parenchyma of a dicotyledonous leaf, obtained in our previous paper,[18] as the model parameters for estimation of the spectral scattering $\beta_{sl}(\lambda)$ and absorption $\beta_{el}(\lambda)$ coefficients, $[\beta_{sl}(\lambda) + \beta_{el}(\lambda) = \beta_l(\lambda)]$ (β_l is the extinction coefficient of a leaf). Since the substantiation is given in detail in Ref. 18, we only note that selection of the dicotyledonous model of the leaf does not violate the generality of results, because such a model is the most characteristic of both wooden and grass vegetation.[17,19]

In its turn, a leaf is approximated as a plane-parallel plate, geometric thickness of which Δh is also a parameter of the problem. As a rule,[19] dicotyledonous leaves contain only two types of the chlorophyll molecules, Chl$_a$ and Chl$_b$. It is difficult to estimate in explicit form relative contributions of the photosystem I (PSI) and photosystem II (PSII) into the spectral intensity of the fluorescence $I_L(\lambda)$ of Chl$_b$ and Chl$_a$, respectively, i.e., neglecting the effect of reabsorption and other factors.[20] The following empirical dependence is proposed[21]:

$$I_L(\lambda) = k_1\mathrm{PSI}(\lambda) + k_2\mathrm{PSII}(\lambda), \qquad (1)$$

where $k_1 = 1$, and $k_2 = 5.85$. According to data from Refs. 20 and 22, w_b = PSI/PSII can vary within $w_b = 0.5–0.7$. Since this parameter determines the processes of reabsorption, it is expedient to include it into the list of parameters.

The absorption and LIF spectra of Chl$_a$ (Fig. 1*a*) and Chl$_b$ (Fig. 1*b*), obtained from the data of photochemical database,[23] are shown in Fig. 1 at a relative scale.

Figure 1*c* shows the range of overlapping of the emission spectrum of Chl$_b$ with the absorption band of Chl$_a$ used in the algorithm of statistical modeling. Optical characteristics of the aerosol atmosphere are described in literature[24] in detail.

2. Mathematical model of the radiation transfer

Let us describe, following Ref. 6, the process of propagation of the lidar signal at the wavelength of the LIF excitation by non-stationary transfer equation (TE) in 3D space $\mathbf{r}(x, y, z)$:

$$\left(\frac{n}{v}\right)\frac{\partial I(\mathbf{r},\Omega,t,\lambda)}{\partial t} + \Omega\nabla I(\mathbf{r},\Omega,t,\lambda) = -\beta_{ext}(\mathbf{r},\lambda)I(\mathbf{r},\Omega,t,\lambda) +$$

$$+\frac{1}{4\pi}\int_{4\pi} G_\Sigma(\mathbf{r},\Omega,t,\lambda)I(\mathbf{r},\Omega',t,\lambda)\mathrm{d}\Omega' + \Phi_0(\mathbf{r},\Omega,t,\lambda), \quad (2)$$

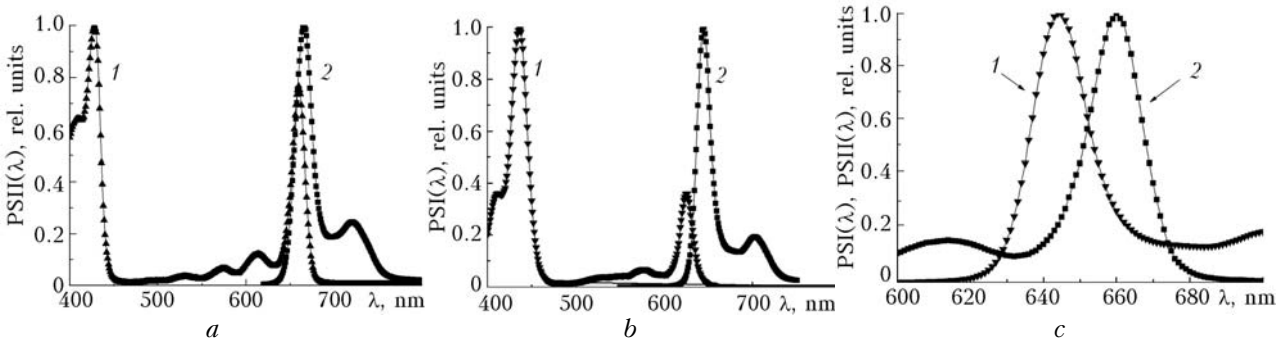

Fig. 1. Absorption (*1*) and fluorescence emission PSII(λ) (*2*) (Chl$_a$) spectra (*a*); absorption (*1*) and fluorescence emission PSII(λ) (*2*) (Chl$_b$) spectra (*b*); normalized fluorescence emission PSI(λ) (Chl$_b$) (*1*) and absorption PSII(λ) (Chl$_a$) (*2*) spectra (*c*).

where $I(\mathbf{r}, \Omega, t, \lambda)$ is the intensity of radiation at λ at the point $\mathbf{r}$ in the direction $\Omega(a, b, c)$; $G_\Sigma(\mathbf{r}, \Omega, t, \lambda)$ is the volume coefficient of the angular elastic scattering by some multi-phase medium; $\beta_{ext}(\lambda)$ is the effective extinction coefficient of the medium at λ, i.e.,

$$\beta_{ext}(\lambda) = \beta_a(\lambda) + \beta_l(\lambda) + \beta_s,$$

$\beta_a(\lambda) = \alpha_A(\lambda) + \beta_{as}(\lambda)$; $\alpha_A(\lambda)$, $\beta_{as}(\lambda)$ are the absorption and scattering coefficients of the aerosol atmosphere, respectively;

$$\beta_l(\lambda) = \alpha_T(\lambda) + \alpha_F(\lambda) + \beta_{sl}(\lambda);$$

α_T is the absorption coefficient of the leaf matter due to heat dissipation; $\alpha_F(\lambda)$ is the absorption by fluorophores; $\beta_{sl}(\lambda)$ is the elastic scattering coefficient; n is the mean refractive index of the leaf matter; v is the light speed in air;

$$G_\Sigma(\mathbf{r},\Omega',\Omega,\lambda) = \sum_i K_i G_i(\mathbf{r},\Omega',\Omega,\lambda). \qquad (3)$$

Here $G_i(\mathbf{r}, \Omega', \Omega, \lambda)$ is the angular elastic scattering coefficient of the ith phase component of the medium; K_i are the weight coefficients (see for detail in Ref. 18).

The extinction coefficient β_s related with the geometric overlapping of the light beam by leaves, by definition, does not depend on the wavelength of the incident radiation and is determined[25] only by the surface density of leaves u_l (m^2/m^3) and the distribution function of the leaf normals Ω_l:

$$\beta_s = \frac{u_l}{2\pi} \int_0^{2\pi} g_l(r,\Omega_l)|\Omega' \cdot \Omega_l| d\Omega_l. \qquad (4)$$

The external source $\Phi_0(\mathbf{r}, t)$ excites fluorophores with the absorption coefficient $\alpha_F(\lambda)$ at the laser radiation wavelength λ. The spectral intensity I_F of the subsequent LIF emission at the wavelength $\lambda' \in \Lambda_F$ (Λ_F is the emission spectral range) satisfies the non-stationary TE:

$$\left(\frac{n}{v}\right)\frac{\partial I_F(\mathbf{r},\Omega,t,\lambda')}{\partial t} + \Omega \nabla I_F(\mathbf{r},\Omega,t,\lambda') =$$

$$= -\beta_{ext}(\mathbf{r},\lambda') I_F(\mathbf{r},\Omega,t,\lambda') +$$

$$+\frac{1}{4\pi}\int_{4\pi} G_\Sigma(\mathbf{r},\Omega',\Omega,\lambda') I_F(\mathbf{r},\Omega',t,\lambda') d\Omega' + \Phi_{L_0}(r,\tau_F,\lambda,\lambda'), \quad (5)$$

where

$$\Phi_{L_0}(r,\tau_F,\lambda,\lambda') = \frac{1}{4\pi}\phi(\lambda')\alpha_F(\lambda) q(\tau_F) \int_{4\pi} I(\mathbf{r},\Omega',t,\lambda) d\Omega'$$

is the function of internal LIF sources, distributed over the volume of the medium. Obviously,[10,26] it depends on the intensity of the exciting radiation, quantum efficiency (quantum yield) of the fluorescence $\phi(\lambda')$, and the decay function

$$q(\tau_F) = \frac{1}{\bar{\tau}_F} \exp\left(-\frac{\tau_F}{\bar{\tau}_F}\right), \qquad (6)$$

where τ_F is the time of the fluorescence decay, $\bar{\tau}_F$ is the mean time of the decay. If the fluorophore I LIF emission spectrum falls in the fluorophore II absorption band, the light quantum at the wavelength λ' is secondary absorbed, and, with some probability, can be reemitted in the emission spectrum of fluorophore II. This is so-called reabsorption process. The spectral intensity I_R of the fluorescent radiation resulting from the reabsorption, satisfies the non-stationary TE of the form

$$\left(\frac{n}{v}\right)\frac{\partial I_R(\mathbf{r},\Omega,t,\lambda'')}{\partial t} + \Omega \nabla I_R(\mathbf{r},\Omega,t,\lambda'') =$$

$$= -\beta_{ext}(\mathbf{r},\lambda'') I_R(\mathbf{r},\Omega,t,\lambda'') +$$

$$+ \frac{1}{4\pi}\int_{4\pi} G_\Sigma(\mathbf{r},\Omega',\Omega,\lambda'') I_R(\mathbf{r},\Omega',\Omega,\lambda'') d\Omega' +$$

$$+\frac{1}{4\pi}\phi(\lambda'')\alpha_F(\lambda') q(\tau_R) \int_{4\pi} I_L(\mathbf{r},\Omega',\tau_F) d\Omega'; \qquad (7)$$

where $\lambda'' \in \Lambda_R$. The function of decay of the secondary emission after reabsorption has somewhat another form:

$$q(\tau_R) = \exp\left[-\xi(\tau_R/\bar{\tau}_R)^{\frac{1}{2}}\right]. \qquad (8)$$

The meaning of τ_R and $\bar{\tau}_R$ is the same as in Eq. (6). Note that mean times of the LIF decay for PSI and PSII essentially differ[20] ($\bar{\tau}_F = 0.1$ and 0.5 ns, respectively).

3. Solution of the system of transfer equations by the Monte Carlo method

The system of non-stationary TE (2), (5), (7) is written in scalar approximation, i.e., neglecting polarization effects. Nevertheless, its rigorous analytical solution for the case of illumination of a multiphase medium by a collimated source seems to be impossible. Among numerical methods, the most rational is the Monte Carlo method.[27,28] It is not necessary to consider the generally accepted elements of the statistical modeling, they are described in detail in the literature.[27,29] Note only some qualitative peculiarities of the algorithm for modeling the effects of reabsorption in comparison to the algorithm used earlier.[6,7]

The first phase of the statistical modeling lies in realization of the Markovian chain of random events, regulated by the core in the generalized integral form (2). In each successive random interaction of a

photon with discrete center of the medium (molecule or particle) its energy can be scattered or absorbed. In the case of occurring the photon inside the leaf volume, the following probability chain is possible:

a) the probability of the event that the photon undergoes the scattering act:

$$P_s(\lambda) = \beta_{sl}(\mathbf{r},\lambda)/\beta_l(\mathbf{r},\lambda); \quad (9)$$

b) the probability of absorption of the photon:

$$P_c(\lambda) = [\alpha_T(\mathbf{r},\lambda) + \alpha_F(\mathbf{r},\lambda)]/\beta_l(\mathbf{r},\lambda); \quad (10)$$

c) the probability of absorption of the photon by fluorophore:

$$P_{cf}(\lambda) = \alpha_F(\mathbf{r},\lambda)/\beta_l(\mathbf{r},\lambda); \quad (11)$$

d) the probability of absorption of the photon by Chl$_b$:

$$P_b = w_b = \mathrm{PSI}/\mathrm{PSII}; \quad (12)$$

e) the probability of the event that the photon, absorbed by Chl$_b$, is reemitted:

$$P_f = \phi(\lambda,\lambda')\alpha_F(\mathbf{r},\lambda)/\beta_l(\mathbf{r},\lambda); \quad (13)$$

f) the probability of the event that $\lambda' \le \lambda_R$, where λ_R is the red boundary of the absorption band of Chl$_a$ (see Fig. 1*c*);

g) the probability of the event that the photon, absorbed by Chl$_a$, is reemitted:

$$P_r = \phi(\lambda',\lambda'')\alpha_F(\mathbf{r},\lambda)/\beta_l(\mathbf{r},\lambda). \quad (14)$$

Note that at this stage we do not consider further processes of energy transfer for donor-acceptor pairs of fluorophores, which are possible in a multi-component medium. Then, when the event (d) is realized, the process of motion with elastic scattering stops.

Thus, the primary photon at the wavelength λ formally governed by TE (2) has a chance to be absorbed by the fluorophore according to Eq. (12). In a certain time interval τ_F, the secondary photon can be emitted with a known probability, as a rule, with a less energy at $\lambda' > \lambda$. Its subsequent history is governed by Eq. (5). New wavelength λ' is selected based on the redistribution function over wavelengths $Y(\nu, \nu')$, set for the particular fluorophore form. In this case (see Fig. 1*a*, *b*), obviously, it can satisfy the relationships:

$$Y(\lambda,\lambda') = \frac{\mathrm{PSI}(\lambda')}{\int\limits_{\Lambda_{\mathrm{PSII}}} \mathrm{PSI}(\lambda')\mathrm{d}\lambda'}$$

or

$$Y(\lambda,\lambda') = \frac{\mathrm{PSII}(\lambda')}{\int\limits_{\Lambda_{\mathrm{PSII}}} \mathrm{PSII}(\lambda')\mathrm{d}\lambda'}, \quad (15)$$

where Λ_{PSI}, Λ_{PSII} are the spectral ranges of emission of photosystems I and II, respectively.

Obviously, the redistribution function $Y(\lambda, \lambda')$ satisfies the condition of normalization.

$$\int_0^\infty Y(\lambda,\lambda')\mathrm{d}\lambda' = 1.$$

If the wavelength of the fluorescent emission λ' of fluorophore I has occurred in the fluorophore II absorption band, the process of reabsorption happens, i.e., the photon is absorbed a second time, and can be reemitted with some probability at the $\lambda'' \ge \lambda'$, $\lambda'' \in \Lambda_R$. Further process of random motion of the photon at λ'' corresponds to TE (7). The redistribution function $Y(\lambda', \lambda'')$ formally has the same form as (15).

As is seen in Figs. 1*a* and *b*, the spectrum of spontaneous LIF can have quite complicated configuration, especially in the case of multi-component medium. The tabulated method of inverse functions[30] is the most effective for modeling such complex inverse functions.

One of the weight methods, so-called "analytical averaging"[27,29] is used for realization of the discrete probability chain (9)–(14), i.e., it is assumed that, during the process of random migration, the photon at the main excitation wavelength λ is always scattered by a particle or a molecule, and its statistical weight $\omega_n(\lambda)$ in the nth collision is reduced by the single scattering albedo $\omega(\lambda)$, i.e.,

$$\omega_n(\lambda) = \omega_{n-1}(\lambda)w(\mathbf{r}',\lambda), \quad \omega_0 = 1 .$$

The weight share $[1 - w(\lambda)]\omega_{n-1}(\lambda)$ remains in the medium as absorbed.

The photon, absorbed by a molecule, following (13), has a certain probability to be reemitted at the fluorescence wavelength λ' selected in the limits of $Y(\lambda, \lambda')$. This probability is determined by the value of the quantum yield $\phi(\lambda, \lambda')$.

$$\omega_n(\lambda') = \omega_{n-1}(\lambda)[1 - w(\lambda)]\phi(\lambda,\lambda').$$

Since data on the spectral dependence $\phi(\lambda, \lambda')$ are not available for the fluorophores, selected for the estimating calculations, but it is known[31] that this dependence is inessential, we assume:

$$\phi(\lambda,\lambda') = \phi = \mathrm{const} \approx 0.01 - 0.05.$$

The angular scattering of the fluorescent photon is, generally speaking, anisotropic, especially when the fluorophore molecules have been included into the matter of aerosol particles.[32] However, since this anisotropy is weakly seen in the approximation of the scalar transfer equation, we also neglect it at the first stage of calculations. The last, quite obvious, assumption is that the secondary fluorescence at λ' and λ'' does not take place. Further random migration of the photon consists of only elastic

collisions. The trajectory breaks at the output of the photon from the medium. According to (6) and (8), spontaneous LIF has a finite time of decay. In the algorithm of the statistical modeling, this leads to additional pathlength of the photon l_n in each collision, accompanied by the fluorescence. This effect will be analyzed in the next paper, although preliminary estimates show that it is minimal on long atmospheric paths.

4. Results of model estimates

Some results of calculations are presented below. They illustrate the efficiency of the proposed algorithms of statistical modeling. As was mentioned above, boundary conditions of the numerical experiment reflected the construction of the real fluorescent lidar operating at the Institute of Atmospheric Optics SB RAS. The receiving-transmitting scheme of the lidar was close to monostatic one, the wavelength of the exciting radiation was $\lambda = 532$ nm, the distance to the homogeneous area of vegetation on a horizontal path was $H_0 = 60$ m; other, less essential in the numerical experiment specifications of the lidar are presented in Refs. 13 and 15.

The important physiological parameter determining the efficiency of appearing reabsorption in the leaf volume is the ratio of the relative content of chlorophylls *a* and *b*, i.e., the relative activity of PSI and PSII (12). In terms of the statistical modeling, this ratio w_b determines the probability of reabsorption. Curves of the spectral intensity of the LIF as functions of the probability w_b are shown in Fig. 2.

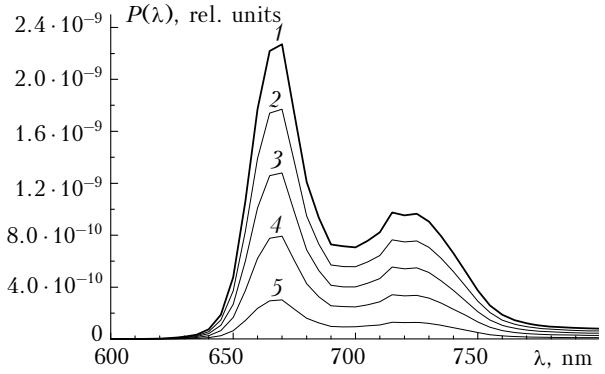

Fig. 2. Spectral dependences of the fluorescence signal on the probability of reabsorption w_b. The leaf thickness $\Delta h = 0.25$ mm. Curves *1–5* correspond to $w_b = 0.1$; 0.3; 0.5; 0.7; 0.9. The angle of receiving $\varphi_d = 1$ mrad.

The calculations were performed at constant value of the total concentration of Chl_a and Chl_b, it is visually obvious that the value of the characteristic ratio I_R/I_{IR} noticeably changes, that qualitatively coincides with the conclusions of Refs. 20 and 21.

The question often appears why the cumbersome mathematical apparatus of the theory of transfer is used for estimation of the radiative characteristics of small-scale phytoelements, for example, a tree leaf. Simple analysis shows that the mean optical thickness of an individual leaf in visible and near IR ranges is comparable with the optical thickness of a small-size individual cumulus cloud. Obviously, the contribution of multiple scattering (integral term of TE) in the leaf volume into characteristics of the optical radar signal should not be underestimated. The optical thickness of a leaf is

$$\tau_l(\lambda) = \int_0^{\Delta h} \beta_l(\lambda, h')\mathrm{d}h' \simeq \beta_{0l}(\lambda)\Delta h,$$

where $\beta_{0l}(\lambda)$ is the mean extinction coefficient over the leaf volume. The pattern of transformation of the spectral behavior of LIF with the increase of the geometric $\Delta h = 0.1$–1.0 mm and, hence, optical thickness of the leaf at constant $w_b = 0.3$ is shown in Fig. 3.

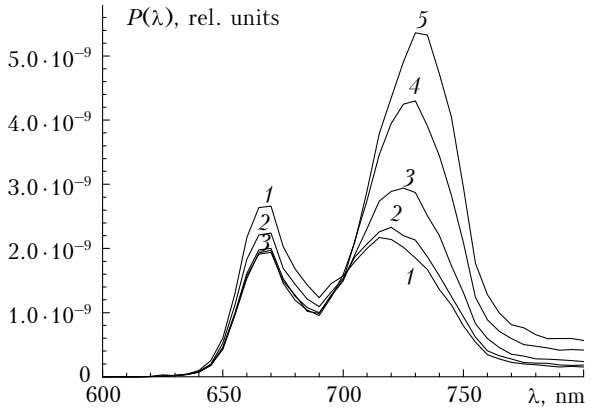

Fig. 3. Spectral dependence of the fluorescence signal on the leaf thickness Δh. Curves *1–5* correspond to $\Delta h = 0.1$; 0.15; 0.25; 0.5; 1 mm. The probability of reabsorption $w_b = 0.3$. The angle of receiving $\varphi_d = 1$ mrad.

High optical thickness of the leaf parenchyma (β_{0l} ($\lambda = 523$ nm) = 8750 m^{-1} [Ref. 18]) leads to the fact that practically all multiple scattering background remains in the limits of the angle of the detector's field of view even at its small values ($\varphi_d = 0.001$ rad). The most essential transformation of the spectrum occurs at $\lambda \geq 710$ nm, where the chlorophyll absorption band terminates. The H_2O absorption band at $\lambda = 760$ nm was neglected in this example. Figure 4 illustrates how the LIF spectrum, recorded on a real atmospheric path, differs from the ideal non-excited spectrum of the spontaneous fluorescence (Chl_a + Chl_b) recorded under laboratory conditions (curve *1′*, [Ref. 23]).

Combined effect of the reabsorption processes and the multiple scattering leads to essential distortion of the own fluorescence spectra of chlorophylls *a* and *b*. When planning the use of detectors based on CCD (charge-coupled device) matrix in combination with a high-speed spectrometer

in further experimental investigations, we have estimated the spatially resolved LIF signal for the same model of the multi-phase medium. The signals of LIF spectral intensity excited by a short δ-pulse of radiation at λ = 532 nm are shown in Fig. 5. The Monte Carlo method enables one to separate the contribution of the pure fluorescent signal free of the background of the multiple scattering; this signal is shown by the dot line.

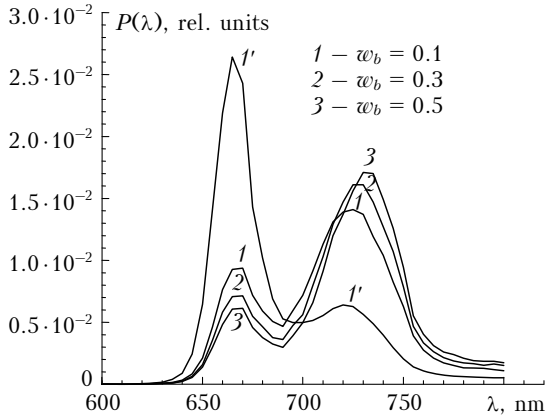

Fig. 4. Model profile of the fluorescence signal (curve *1′*) and the normalized integral LIF signal (*1–3*) as functions of probability of reabsorption w_b = 0.1; 0.3; 0.5, respectively. The angle of receiving φ_d = 1 mrad.

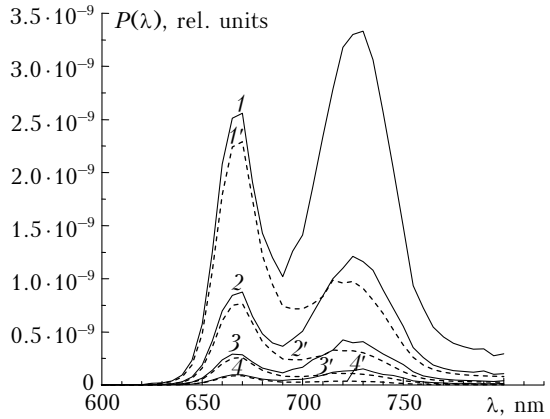

Fig. 5. The effect of the multiple scattering background on the level of the LIF signal coming from the depth H = 2.5; 5.0; 7.5; and 10 m, respectively (curves *1–4*). Curves *1′–4′* show the fluorescence signal. The leaf thickness Δh = 0.25 mm; the probability of reabsorption w_b = 0.3; φ_d = 1 mrad.

Note that the energy level of the LIF signal dramatically decreases at the distance of several meters, the shape of the spectrum is noticeably distorted, and the significant background of the multiple scattering remains.

Conclusions

Estimates of the spectral intensity of the laser-induced fluorescence in the scheme of lidar sensing of the vegetation cover, carried out on the basis of rigorous radiative approach, have shown that simple empirical approach to monitoring of the chlorophyll concentration based on measurements of I_R/I_{IR}, can lead to essentially shifted results. It is revealed that the reason of this shift can be the processes of the LIF re-absorption and multiple scattering, resulting in a significant transformation of the fluorescence spectra, especially in the near IR range.

Acknowledgements

This work was supported in part by Russian Foundation for Basic Research (Grants Nos. 06-05-64799, 06-05-96962, and 07-01-00509).

References

1. D.V. Pozdnyakov, A.V. Lyaskovskii, H. Grassl, and L. Petterson, Issled. Zemli iz Kosmosa, No. 5, 3–15 (2000).
2. S. Sathyendranath and T. Platt, Appl. Opt. **37**, 2216–2227 (1998)
3. S.H. Melfi, Appl. Opt. **11**, 1605–1610 (1972).
4. C. Weitkamp, ed., *Lidar: Range – Resolved Optical Remote Sensing of the Atmospheric* (Singapore, Springer Science + Business Media Inc, 2005), 451 pp.
5. R.M. Measures, *Laser Remote Sensing* (Join Wiley and Sons, New York, 1987).
6. G.M. Krekov and M.M. Krekova, Atmos. Oceanic Opt. **20**, No. 2, 134–140 (2007).
7. G.M. Krekov, M.M. Krekova, G.G. Matvienko, A.V. Kovshov, and A.Ya. Sukhanov, Atmos. Oceanic Opt. **20**, No. 3, 237–247 (2007)
8. K.Ya. Kondratyev and D.V. Pozdnyakov, *Optical Properties of Natural Waters and Remote Sensing of Phytoplankton* (Nauka, Leningrad, 1988), 183 pp.
9. Y. Saito, M. Kanoh, K. Hatake, T. Kawahara, and A. Nomura, Appl. Opt. **37**, 431–437 (1998)
10. G.C. Papageorgiou, ed., *Chlorophyll a Fluorescence: a Signature of Photosynthesis* (Springer, The Netherlands, 2004), 735 pp.
11. G.B. Cordon and M.G. Lagorio, Photochem. Photobiol. Sci. **5**, 735–740 (2006)
12. T. Renger, V. May, and O. Kuhn, Phys. Reports **343**, 137–254 (2001).
13. A.I. Grishin, G.M. Krekov, M.M. Krekova, G.G. Matvienko, A.Ja. Sukhanov, N.L. Fateeva, and V.I. Timofeev, Int. J. Remote Sens. **29**, No. 9 (2008) (in press).
14. A. Harriman, Photochem. **32**, 15–46 (2001).
15. A.I. Grishin, G.M. Krekov, M.M. Krekova, G.G. Matvienko, A.Ya. Sukhanov, V.I. Timofeev, N.L. Fateyeva, and A.A. Lisenko, Atmos. Oceanic Opt. **20**, No. 4, 294–302 (2007)
16. G.M. Krekov, M.M. Krekova, and G.G. Matvienko, in: *Proc. XIII Int. Sympos. "Atmospheric Oceanic Optics,"* Tomsk (2006), pp. 127–128.
17. Y.M. Govaerts, S. Jacquemoud, M.M. Verstraete, and S.L. Ustin, Appl. Opt. **35**, No. 33, 6575–6578 (1996).
18. G.M. Krekov, M.M. Krekova, A.V. Kovshov, A.A. Lisenko, and A.Ya. Sukhanov, Atmos. Oceanic Opt. **22** (2009) (in press).
19. S.L. Ustin, S. Jacquemoud, and Y.M. Govaerts, Plant, Cell and Environ. **24**, 1095–1103 (2001)
20. R. Pedrros, I. Moya, Y. Goulas, and S. Jacquemoud Photochem. Photobiol. Sci. **7**, 498–502 (2008).
21. F. Franck, P. Juneau, and R. Popovic, Biochim. Biophys. Acta **1556**, 239–246 (2002)

22. D.Y. Fan, A.B. Hope, and P.J. Smith, Biochim. Biophys. Acta **1767**, 1064–1072 (2007)
23. http://www.photochemcad.com
24. V.E. Zuev and G.M. Krekov, *Optical Models of the Atmosphere* (Gidrometeoizdat, Leningrad, 1986), 256 pp.
25. Y.V. Knyazikhin, A.L. Marshak, and R.B. Myneni, Remote Sens. Environ. **39**, 61–74 (1992).
26. D.Y. Paithakar, A.U. Chen, B.W. Pogue, M.S. Patterson, and E.M. Sevick-Muraca, Appl. Opt. **36**, 2260–2272 (1997).
27. G.I. Marchuk, ed., *Monte Carlo Method in Atmospheric Optics* (Heidelberg: Springer-Verlag, Berlin, 1980), 206 pp.
28. H. Greenspan, ed., *Computing Method in Reactor Physics* (Gordon and Breach Sci., New York, London, Paris, 1972), 372 pp.
29. G.M. Krekov, V.M. Orlov, V.V. Belov, and M.L. Belov, *Imitation Modeling in the Problems of Optical Remote Sensing* (Nauka, Novosibirsk, 1988), 164 pp.
30. G.M. Krekov and L.G. Shamanaeva, in: *Atmospheric Optics* (Nauka, Moscow, 1974), pp. 180–186.
31. G. Lakovich, *Principles of Fluorescent Spectroscopy* (Mir, Moscow, 1986), 496 pp.
32. H. Chew, P.J. MeNulty, and M. Kerker, Phys. Rev. Lett. **85**, 54–57 (2000).